Journal of
Pharmaceutical and BioTech Industry

MDPI

Article

The Formulation, Preparation, and Evaluation of Celecoxib Nanosuspensions: Nanosizing via High-Pressure Homogenization and Conversion of the Nanosuspensions into Dry Powders by Spray Drying and Freeze Drying

Rukesh Machamasi [1,2,†], Sung-Joo Hwang [1,2,*] and Linh Dinh [3,*,†]

[1] College of Pharmacy, Yonsei University, 85 Songdogwahak-ro, Yeonsu-gu, Incheon 21983, Republic of Korea; machamasirukesh@gmail.com
[2] Yonsei Institute of Pharmaceutical Sciences, Yonsei University, 85 Songdogwahak-ro, Yeonsu-gu, Incheon 21983, Republic of Korea
[3] Division of Pharmaceutical Sciences, James L. Winkle College of Pharmacy, University of Cincinnati, Cincinnati, OH 45229, USA
* Correspondence: sjh11@yonsei.ac.kr (S.-J.H.); dinhlk@ucmail.uc.edu (L.D.)
† These authors contributed equally to this work.

Abstract: Celecoxib (CEL), a nonsteroidal anti-inflammation drug (NSAID), is categorized as a Class II drug (low solubility, high permeability) in the Biopharmaceutics Classification System (BCS). The aim of this study is to develop a novel formulation of CEL nanosuspensions in the form of dried powder for tableting or capsuling. In this study, CEL was formulated into nanosuspensions to improve its solubility. CEL nanosuspensions were prepared using the precipitation method followed by high-pressure homogenization. Drying of the nanosuspensions was performed by spray drying and freeze drying. We examined the impact of various formulation and processing parameters on the nanoparticles. The CEL nanoparticles were characterized by particle size analysis, differential scanning calorimetry (DSC), powder X-Ray diffraction (PXRD), attenuated total reflectance Fourier transform infrared spectroscopy (ATR-FTIR), and dissolution tests. The choice of solvent, stabilizer, and surfactant appeared to have significant impacts on the crystallization and particle size and, consequently, the solubility of the CEL nanoparticles. CEL chemical stability was maintained throughout both drying processes. Both spray-dried and freeze-dried CEL nanosuspensions showed rapid dissolution profiles compared to raw CEL due to the nanosized particle dispersion with the presence of a lag phase. The freeze-dried nanosuspension showed a slight delay in the first 20 min compared to the spray-dried nanosuspension, after which dissolution progressed with a lag phase that represents aggregation.

Keywords: celecoxib; nanosuspension; high-pressure homogenization; spray drying; freeze drying

Citation: Machamasi, R.; Hwang, S.-J.; Dinh, L. The Formulation, Preparation, and Evaluation of Celecoxib Nanosuspensions: Nanosizing via High-Pressure Homogenization and Conversion of the Nanosuspensions into Dry Powders by Spray Drying and Freeze Drying. *J. Pharm. BioTech Ind.* **2024**, *1*, 20–37. https://doi.org/10.3390/jpbi1010004

Academic Editor: Robert Ancuceanu

Received: 15 October 2024
Revised: 6 December 2024
Accepted: 10 December 2024
Published: 12 December 2024

1. Introduction

Celecoxib (CEL), a nonsteroidal anti-inflammatory drug (NSAID), is highly effective in reducing pain and inflammation, with a significant and growing market. Unlike non-selective NSAIDs, CEL selectively inhibits the cyclooxygenase-2 (COX-2) enzyme, which helps reduce the risk of gastrointestinal side effects [1,2]. CEL is widely available and affordable, making it a versatile medication for healthcare providers. CEL is widely prescribed to treat a variety of conditions including arthritis, menstrual cramps, and dental procedures. Additionally, researchers are interested in investigating whether CEL could be used to treat other conditions besides pain and inflammation [3]. Our study aims to improve CEL formulations; by developing improved formulations of CEL, we hope to enhance its efficacy and patient tolerability. Previously, we succeeded in preparing intramuscularly long-acting CEL nanosuspensions for postoperative pain management,

thus exploring CEL's potential new applications [1]. Although CEL can be formulated for different routes of administration, oral administration is the most popular route of administration for CEL [2,4]. CEL is commonly available in capsules which are typically filled with CEL powder [4]. The aim of this study is to develop a novel formulation of CEL nanosuspensions in the form of dried powder for tableting or capsuling, providing a convenient and patient-friendly dosage form. By converting CEL nanosuspensions into a dry powder, we aim to overcome the challenges associated with liquid formulations, such as stability and ease of administration.

CEL is categorized as a Class II drug (low solubility, high permeability) in the Biopharmaceutics Classification System (BCS). The hydrophobicity (log P = 3.5) and extremely poor water solubility (3–7 μg/mL) of CEL make its oral administration difficult, resulting in high variability in absorption [4,5]. Multiple formulations were developed to improve CEL's solubility and dissolution characteristics [1,4–6]. In recent years, scientists have used a variety of approaches to solve the issue of poor solubility, and the nanotechnology process has been recognized as a promising approach for enhancing drug solubility. Nanonization increases the contact surface area, speeding up the dissolution rate and enhancing solubility [7]. There are techniques available to produce reduced particle-size drugs including precipitation [1], solid dispersions [8], microemulsions [9], liposomes [10], micellar systems [11], and nanosuspensions [1]. Nanotechnology exhibits superior performance for poorly soluble drugs, enhancing the loading capacity, oral absorption consistency, and bioavailability [12]. There are two ways to prepare nanosuspensions: (1) the top–down approach and (2) the bottom–up approach. High-pressure homogenization technology is considered a typical top–down approach in which mechanical abrasion breaks down the larger particles into smaller particles. On the other hand, the antisolvent precipitation method is a bottom–up approach in which particles solubilized in the organic solvent are quickly added to the inorganic phase, resulting in drug precipitation under supersaturated conditions [13]. Functioning as an efficient and dependable aqueous-insoluble drug delivery system, nanosuspensions bring about an augmented surface-to-volume ratio. This enhancement facilitates improved interaction with the medium, thereby enhancing drug solubility. The prospective advancement of nanosuspensions as a feasible technique aims to optimize and revitalize present marketed drugs with insufficient delivery mechanisms, yielding enhanced benefits clinically as well as commercially. Furthermore, nanosuspensions have an advantage since they can be formulated as suspensions or as solid dosage forms through drying [14].

In this study, CEL nanosuspensions were prepared via the combination of nanoprecipitation–homogenization, followed by drying for the conversion of the CEL nanosuspension to dry powder. Drying of the nanosuspensions was performed by (1) spray drying and (2) freeze drying. The impact of the drying process on the dry powder is herein discussed. While the focus of this article is on the formulation and preparation of CEL nanosuspensions, we take into consideration the drying conditions and techniques as well as the dispersibility of the dried nanoparticles and the subsequent dry powdered CEL nanoparticles for oral dosage forms.

2. Materials and Methods

2.1. Materials

The CEL manufactured by Pfizer, Inc. (New York, NY, USA) was a kind gift from the DaeHwa Pharmaceuticals Co., Ltd. (Koonsan, Gangwon-do, Republic of Korea). Isopropyl alcohol (IPA), propylene glycol, and polysorbate 80 were purchased from Dae Jung Chemicals and Metals Co., Ltd. (Siheung, Gyeonggi-do, Republic of Korea). Acetone, trifluoroacetic acid (TFA), ethyl acetate, sodium lauryl sulfate (SLS), and hydrochloric acid (HCl) were purchased from Samchun Pure Chemical Co., Ltd. (Pyeongtaek, Gyeonggi-do, Republic of Korea). Methanol and acetonitrile (ACN) were purchased from Avantor Performance Materials (Radnor, PA, USA). Polyvinylpyrrolidone K 12 (PVP K 12) and polyvinylpyrrolidone K 30 (PVP K 30) were purchased from BASF Chemical Company

(Ludwigshafen, Germany). Polyvinyl alcohol (86% hydrolyzed) (PVA) and 2 hydroxyl propyl-β cyclodextrin (β-cyclodextrin) were purchased from Sigma-Aldrich (St. Louis, MO, USA). Hydroxypropyl methylcellulose K 15 M (HPMC) was purchased from Colorcon, Inc., (Bucgwiese, Germany). Ethanol was purchased from Duksan Pure Chemicals (Ansan, Gyeonggi-do, Republic of Korea). Water was purified and dispensed from the Wasserlab Autwomatic Plus 1+2 GR system (Pamplona, Spain).

2.2. Methods

2.2.1. Solubility Study

The solubility study of CEL in water and various solvents (water, ethanol, methanol, IPA, ACN, acetone, and ethyl acetate) was carried out at room temperature (25 °C). Briefly, 1 mg of CEL was added to 1 mL of solvent in a 1.5 mL Eppendorf® tube. Then, an excess amount of CEL (equivalent to 1 mg) was added repeatedly followed by vortexing (Vortex-Genie 2, Scientific Industries, Inc., Bohemia, NY, USA) for 1 min. The sample was checked visually for any undissolved insoluble solute. Once saturation was reached, the tube was placed in a rotator mixer (CRT-350 Rotator; Lab Companion, Daejeon, Republic of Korea) at 50 rpm for 72 h at room temperature. After 72 h, the samples were centrifuged at 10,000 rpm for 10 min using a microcentrifuge (Hanil M15R; Hanil Scientific Inc., Gimpo, Gyeonggi-do, Republic of Korea). Then, the supernatant was collected. The collected supernatant was diluted using a solution of 0.2% TFA: ACN (30:70 v/v), filtered with a 0.2 µm Whatman™ Pura-disc™ non-sterile polytetrafluoroethylene (PTFE) syringe filter (Whatman plc, Maidstone, UK), and analyzed by high-performance liquid chromatography (HPLC) for CEL content. The HPLC assay was performed using the Agilent-HPLC system 1200 infinity series (Agilent Technologies, Waldbronn, Germany), with a C_{18} column (CAPCELL, 120 Å pore size, 5 mm, 4.6 mm inside diameter × 250 mm; Shishedo, Tokyo, Japan). The column temperature was set at 25 °C. The mobile phase comprised 0.2% TFA and ACN in a ratio of 30:70 v/v, pumped at a rate of 1.2 mL/min. TFA was used as an ion processing agent in reverse-phase chromatography to improve peak shape and resolution because the silica used in the column may contain metal ion impurities. The absorption wavelength was set at 258 nm. The retention time was approximately 3.5 min. The amounts of CEL were then calculated based on the standard calibration curve obtained for CEL in the same condition. The samples were measured in triplicate (n = 3).

Solubility measurements of CEL in PVA, PVP K12, PVP K30, HPMC, and β-cyclodextrin were carried out at room temperature (25 °C). A polymer solution was prepared by weighing 1 g of the polymer solute and then dissolving it in 100 mL of water. Briefly, 20 mg of CEL was added to a 15 mL conical tube containing 10 mg/mL of the polymer solution. Then, 10 mg of PVP K12 or PVP K30 was added repeatedly followed by vortexing for 5 min and sonicating for 15 min. The samples were checked visually for any insolubility or precipitation and placed in a water bath at 50 rpm for 72 h. After 72 h, the samples were centrifuged at 10,000 rpm for 10 min. Then, the supernatant was collected. The collected supernatant was diluted using a solution of ACN:0.2% TFA (70:30 v/v), filtered with a 0.2 µm Whatman™ Pura-disc™ non-sterile PTFE syringe filter, and analyzed by HPLC for CEL content. The samples were measured in triplicate (n = 3).

2.2.2. Preparation of CEL Nanosuspensions

Nanoprecipitation

CEL nanosuspensions were produced via the solvent exchange method by adding the CEL solution dropwise into an antisolvent phase (10 mg/mL polymeric solution) and stirring using a magnetic stirrer at 400 rpm for 1 h.

Particle size analysis of the suspension was conducted using a dynamic light scattering (DLS) instrument (Lifesizer 500, Anton Paar GmbH, Graz, Austria). The suspension was added to a rectangular sample cell to obtain transmittance for the measurement. A relative refractive index value of 1.2 was used for particle size analysis. Diffracted light was situated at a 90° orientation. The samples were measured at 25 °C in triplicate (n = 3).

High-Pressure Homogenization

The CEL suspensions were passed through a Nanodebee high-pressure homogenizer (Bee International, South Easton, MA, USA) set at 1500 psi for 5 cycles. Particle size analysis was performed.

2.2.3. Preparation of Dry Powdered CEL Nanoparticles

Spray Drying

The spray-drying process was conducted using a SD1000 spray-drying unit (Eyela, Tokyo, Japan), equipped with thermocouples for inlet and outlet temperatures and controllers for pump and aspiration rates. The spray dryer was equilibrated with water prior to every run. A typical batch size for spray drying was around 400 mL (feeding volume). The CEL nanosuspension was pumped into the spray-drying chamber. Spray drying was conducted at an inlet temperature of 135 °C under an atomization pressure of 10 × 10 kPa with a blowing rate of 0.26 m^3/min. A sieving step was performed to obtain a fine powder.

Freeze Drying (Lyophilization)

A volume of 400 mL of each prepared CEL nanosuspension was subjected to lyophilization using a Lyoph-Pride SCM unit (ilShin Biobase, Dongducheon, Gyeonggi-do, Republic of Korea) at −80 °C ± 1.0 °C for 12 h under vacuum (5 mTorr). A sieving step was performed to obtain a fine powder.

2.2.4. Differential Scanning Calorimetry (DSC)

The thermal properties of the raw CEL as well as the selected formulations were assessed by using the DSC Q 2000 instrument (TA instrument, New Castle, DE, USA). For spray-dried and freeze-dried CEL nanoparticles and raw CEL powder, 2–5 mg of each sample was weighed accurately in a T-zero aluminum pan which was properly sealed with a lid. An empty pan was prepared and sealed for reference purposes. Analysis was performed between 40 °C and 180 °C at a 10 °C/min heating rate under a nitrogen flow of 40 mL/min.

2.2.5. Attenuated Total Reflectance Fourier Transform Infrared (ATR-FTIR) Spectroscopy

Infrared spectra of the samples were recorded using the Cary 670 FTIR spectrometer (Agilent Technologies, Santa Clara, CA, USA) equipped with an attenuated total reflectance (ZnSe crystal). Each spectrum was scanned in the range of 400–4000 cm^{-1} with a resolution of 8 cm^{-1} and was derived from single average scans collected in the mid-infrared region (2.5 to 50 μm) at a high spectral resolution; a total of 32 scans were obtained.

2.2.6. Powder X-Ray Diffraction (PXRD)

A Rigaku smart LAB X-Ray diffraction system (Rigaku, Tokyo, Japan) in the θ/2θ scan mode using Cu-Kα radiation was used to measure PXRD patterns of the samples under the setting of the diffraction pattern in a 2θ range of 3–60° with a step size of 0.02° and a scanning speed of 4°/min.

2.2.7. Scanning Electron Microscopy (SEM)

The size, shape, and surface of the dry powdered raw CEL and CEL nanoparticles were determined by scanning electron microscopy (SEM) (JSM-7800F, JEOL, Tokyo, Japan). Briefly, an amount of powder (typically around 5–10 mg) was sprinkled onto adhesive carbon tape (Ted Pella Inc., Redding, CA, USA), where the excess powder was gently removed by a jet. The samples were then attached to an aluminum stub and were sputter-coated with gold under vacuum. Photographs were taken at 2700× magnification with a voltage of 10 kV to reveal the surface characteristics of the particles.

2.2.8. Dissolution Test

The wettability of dry powders impacts dispersibility and dissolution. The powdered samples were mixed in dissolution media for 5 min at 37 °C to allow for thorough wetting of the particles. The wetting process can be considered the initial part of the gastrointestinal transit of the oral solid dosage form, wherein the dosage form disintegrates to allow the particles to come in contact with the aqueous medium [15].

Dissolution studies were carried out in an automated dissolution tester (DISTEC 2500, Distek Inc., North Brunswick, NJ, USA) using the USP Apparatus 2 (paddle) method. The bath temperature and paddle speed were set at 37 °C and 50 rpm, respectively. The dissolution test was performed in 2 types of dissolution media: (1) 0.1 M HCl with 0.2% SLS and (2) 0.1 M HCl. The gastrointestinal fluid acidic condition was imitated, and SLS was used as the presence of bile salts and other surfactants in the gastrointestinal tract. Including SLS in dissolution testing is considered more physiological and reflective of the conditions under which the drug is intended to be absorbed in the body [1,16]. A certain weight of samples equivalent to 100 mg CEL was capsulated, put inside a basket (sinker) and then put into the vessels filled with 900 mL of dissolution media. Samples of dissolution medium (1 mL) were withdrawn through a filter at designated time points: t = 5, 10, 15, 20, 30, 45, 60, 90, and 120 min. After a volume of 1 mL was retrieved from the dissolution apparatus, concurrently, 1 mL of the fresh medium was introduced to the dissolution media. The samples were assayed for CEL concentration using HPLC. The dissolution of each sample was determined in triplicate (n = 3).

Statistical Analysis

Statistical analyses were carried out using Excel (Microsoft) and Origin 2023 (10.0) software.

3. Results and Discussion

3.1. Solubility Study

Table 1 shows the solubility of CEL in the studied solvents. The solubility of CEL in water was 0.002 mg/mL at room temperature. In agreement with our finding, the aqueous solubility of CEL is reported as 3–7 µg/mL at pH 7 and 37 °C [17]. Propylene glycol, IPA, ethanol, methanol, acetone, ACN, and ethyl acetate showed their capability to dissolve CEL sufficiently. In the studied solvents, the solubility decreases in the order of acetone > ethyl acetate > ACN > methanol > ethanol > IPA > propylene glycol. In this study, an ideal organic solvent for nanosuspension preparation should have several advantageous properties including polarity, miscibility with water, volatility, and biodegradability. Propylene glycol, ethanol, and ethyl acetate are organic compounds that can be administered orally with relatively low toxicity. We did not choose propylene glycol due to its high viscosity and low volatility. Although ethyl acetate is generally considered to have low toxicity, the consumption of ethyl acetate can lead to gastrointestinal distress due to its slow rate of absorption from the gastrointestinal tract [18]. Ethanol was selected as the solvent for the preparation of CEL nanosuspensions for oral administration.

Table 1 shows the solubility of CEL in PVP K30, PVP K12, PVA, HPMC, and β-cyclodextrin at different stabilizer-to-CEL ratios. CEL remains practically insoluble in the studied polymers. In the studied polymeric solutions prepared at 10% w/w, the solubility increases in the order of HPMC < PVA < PVP K30 < PVP K12 < β-cyclodextrin. CEL solubility in β-cyclodextrin was the highest among the studied polymers. Interestingly, increasing the β-cyclodextrin-to-CEL ratios enhanced the amount of CEL dissolved, respectively. While this is a well-known effect of inclusion compound formation, a phase solubility study would be very enlightening.

Table 1. Solubility study.

	Solvent	Note	Solubility (mg/mL) *
Solvent screening	Water		0.002 ± 0.001
	Propylene glycol	Low volatility	36.49 ± 5.934
	IPA	High toxicity	49.16 ± 6.102
	Ethanol		92.34 ± 3.889
	Methanol	High toxicity	181.45 ± 12.510
	Acetone	High toxicity	607.05 ± 8.894
	CAN	High toxicity	
	Ethyl acetate		355.91 ± 20.184
Polymer screening	PVP K 30 10% *w*/*w*	CEL: PVP K 30 *w*/*w* ratio = 1:1	0.033 ± 0.002
		CEL: PVP K 30 *w*/*w* ratio = 1:2	0.024 ± 0.001
		CEL: PVP K 30 *w*/*w* ratio = 1:3	0.003 ± 0.001
	PVP K 12 10% *w*/*w*	CEL: PVP K 12 *w*/*w* ratio = 1:1	0.031 ± 0.002
		CEL: PVP K 12 *w*/*w* ratio = 1:2	0.022 ± 0.002
		CEL: PVP K 12 *w*/*w* ratio = 1:3	0.014 ± 0.001
	PVA 10% *w*/*w*	CEL: PVA *w*/*w* ratio = 1:1	0.001 ± 0.001
		CEL: PVA *w*/*w* ratio = 1:2	0.017 ± 0.001
		CEL: PVA *w*/*w* ratio = 1:3	0.036 ± 0.002
	HPMC 10% *w*/*w*	CEL: HPMC *w*/*w* ratio = 1:1	0.008± 0.002
		CEL: HPMC *w*/*w* ratio = 1:2	0.003 ± 0.001
		CEL: HPMC *w*/*w* ratio = 1:3	0.002 ± 0.001
	β-cyclodextrin 10% *w*/*w*	CEL: β-cyclodextrin *w*/*w* ratio = 1:1	0.051± 0.002
		CEL: β-cyclodextrin *w*/*w* ratio = 1:2	0.067 ± 0.003
		CEL: β-cyclodextrin *w*/*w* ratio = 1:3	0.104 ± 0.002

* Data are presented as mean ± standard deviation.

3.2. CEL Nanosuspensions

Briefly, CEL dissolved in ethanol (solvent) was added dropwise into an aqueous solution containing stabilizers (PVP K30, PVP K12, PVA, HPMC, and β-cyclodextrin) and surfactants (SLS and Tween 80) (antisolvent) at different ratios, and then the mixture was stirred with a magnetic stirrer at 400 rpm and placed in an ultrasonic water bath for 5 min of sonication. The obtained mixture was continuously stirred for 30 min to obtain a coarse suspension. Table 2 shows the composition of the prepared CEL coarse suspensions and their particle size results. The studied stabilizers can influence particle size depending on the solubility; for example, β-cyclodextrin improves the solubility of poorly soluble CEL, resulting in a low particle size, but an excess amount of β-cyclodextrin can form inclusion complexes with Tween 80, increasing particle size [19]. While stabilizers and surfactants are often used in combination, the interaction between stabilizers and surfactants can significantly influence particle size. While CEL is practically insoluble in PVA, adding hydrophobic Tween 80 helps solubilize CEL, making CEL more compatible with the aqueous polymeric environment, thus preventing precipitation and maintaining a smaller particle size. In addition, PVP can form a protective coating around particles, often resulting in bigger particles [20]. Higher concentrations of polymers may lead to a stronger binding effect, which can cause aggregation. The effect seen among the different formulations might not only be the effect of aggregation, but also the differences which mainly depend on the type of polymer that CEL was co-precipitated with. PVP and β-cyclodextrin are extremely soluble in water at room temperature, while HPMC and PVA might need a longer time of contact or higher temperatures to be fully dissolved, thus prolonging the time needed for CEL to dissolve into the solution.

Table 2. CEL coarse suspensions.

CEL Suspensions								Particle Size (μm) *
Ethanol	Antisolvent							
	Stabilizer						Surfactant	
CEL (mg)	PVP K 30 (mg)	PVP K 12 (mg)	PVA (mg)	HPMC (mg)	β-Cyclodextrin (mg)	SLS (mg)	Tween 80 (mg)	
20	20	-	-	-	-	-	-	55.93 ± 2.98
20	-	20	-	-	-	-	-	19.96 ± 14.46
20	-	-	20	-	-	-	-	20.28 ± 2.08
20	-	-	-	20	-	-	-	22.51 ± 3.21
20	-	-	-	-	20	-	-	25.56 ± 4.44
20	20	-	-	-	-	20	-	5.64 ± 3.00
20	20	-	-	-	-	-	20	8.51 ± 1.50
20	-	20	-	-	-	20	-	12.05 ± 1.16
20	-	20	-	-	-	-	20	10.92 ± 3.49
20	-	-	20	-	-	20	-	37.46 ± 4.46
20	-	-	20	-	-	-	20	19.43 ± 6.05
20	-	-	-	20	-	20	-	6.69 ± 4.31
20	-	-	-	20	-	-	20	9.24 ± 1.24
20	-	-	-	-	20	20	-	2.05 ± 0.91
20	-	-	-	-	20	-	20	28.15 ± 2.15
20	20	-	-	-	-	40	-	7.15 ± 2.59
20	20	-	-	-	-	-	40	6.13 ± 0.42
20	-	20	-	-	-	40	-	8.38 ± 1.96
20	-	20	-	-	-	-	40	17.71 ± 1.07
20	-	-	20	-	-	40	-	35.13 ± 15.16
20	-	-	20	-	-	-	40	3.95 ± 1.68
20	-	-	-	20	-	40	-	13.05 ± 4.97
20	-	-	-	20	-	-	40	22.52 ± 2.90
20	-	-	-	-	20	40	-	5.23 ± 3.05
20	-	-	-	-	20	-	40	5.72 ± 0.91
20	40	-	-	-	-	40	-	8.43 ± 4.15
20	40	-	-	-	-	-	40	6.83 ± 2.73
20	-	40	-	-	-	40	-	4.21 ± 1.81
20	-	40	-	-	-	-	40	15.45 ± 6.33
20	-	-	40	-	-	40	-	7.96 ± 1.24
20	-	-	40	-	-	-	40	10.79 ± 6.58
20	-	-	-	40	-	40	-	12.21 ± 5.48
20	-	-	-	40	-	-	40	4.57 ± 4.00
20	-	-	-	-	40	40	-	5.06 ± 4.34
20	-	-	-	-	40	-	40	17.63 ± 2.60
20	40	-	-	-	-	20	-	71.73 ± 6.12

Table 2. *Cont.*

CEL Suspensions								Particle Size (μm) *
Ethanol	Antisolvent							
	Stabilizer						Surfactant	
CEL (mg)	PVP K 30 (mg)	PVP K 12 (mg)	PVA (mg)	HPMC (mg)	β-Cyclodextrin (mg)	SLS (mg)	Tween 80 (mg)	
20	40	-	-	-	-	-	20	30.86 ± 4.14
20	-	40	-	-	-	20	-	14.34 ± 8.52
20	-	40	-	-	-	-	20	6.97 ± 1.15
20	-	-	40	-	-	20	-	23.01 ± 2.52
20	-	-	40	-	-	-	20	13.61 ± 1.18
20	-	-	-	40	-	20	-	7.55 ± 3.11
20	-	-	-	40	-	-	20	6.67 ± 2.63
20	-	-	-	-	40	20	-	5.68 ± 2.56
20	-	-	-	-	40	-	20	30.8 ± 3.35
20	40	-	-	-	-	-	-	53.78 ± 4.29
20	-	40	-	-	-	-	-	12.75 ± 1.64
20	-	-	40	-	-	-	-	14.02 ± 11.75
20	-	-	-	40	-	-	-	15.87 ± 1.98
20	-	-	-	-	40	-	-	22.95 ± 11.96
20		80	-	-	-	-	-	19.58 ± 7.49
20		-	80	-	-	-	-	17.87 ± 2.28
20		-	-	80	-	-	-	11.62 ± 1.50
20		-	-	-	80	-	-	16.83 ± 1.50
20		-	-	-	-	80	-	7.94 ± 4.43
20	80	-	-	-	-	20	-	29.56 ± 3.10
20	80	-	-	-	-	-	20	12.54 ± 8.61
20	-	80	-	-	-	20	-	5.13 ± 0.91
20	-	80	-	-	-	-	20	7.23 ± 1.01
20	-	-	80	-	-	20	-	13.01 ± 0.73
20	-	-	80	-	-	-	20	5.58 ± 2.19
20	-	-	-	80	-	20	-	31.76 ± 4.08
20	-	-	-	80	-	-	20	6.56 ± 1.68
20	-	-	-	-	80	20	-	4.5 ± 1.29
20	-	-	-	-	80	-	20	35.94 ± 2.91
20	80	-	-	-	-	40	-	10.89 ± 4.75
20	80	-	-	-	-	-	40	6.64 ± 0.57
20	-	80	-	-	-	40	-	4.21 ± 1.81
20	-	80	-	-	-	-	40	15.45 ± 6.33

Table 2. *Cont.*

CEL Suspensions								
Ethanol	**Antisolvent**							**Particle Size (μm) ***
	Stabilizer						**Surfactant**	
CEL (mg)	**PVP K 30 (mg)**	**PVP K 12 (mg)**	**PVA (mg)**	**HPMC (mg)**	**β-Cyclodextrin (mg)**	**SLS (mg)**	**Tween 80 (mg)**	
20	-	-	80	-	-	40	-	12.15 ± 3.05
20	-	-	80	-	-	-	40	18.65 ± 11.12
20	-	-	-	80	-	40	-	8.72 ± 6.97
20	-	-	-	80	-	-	40	3.30 ± 1.24
20	-	-	-	-	80	40	-	22.87 ± 2.03
20	-	-	-	-	80	-	40	6.07 ± 1.83

* Data are presented as mean ± standard deviation.

According to the early screening results (Table 2), formulations that exhibited the lowest particle size values were prepared and then subjected to the high-pressure homogenization process. Ostwald ripening tendency was tested by exposing the formulations to high-temperature conditions. Aggregation tendency was tested by putting the formulations in a shaking water bath. Stable CEL nanosuspensions without the visible presence of aggregate, cake, or Ostwald ripening are listed in Table 3. These nanosuspensions were further transformed to powder by spray drying or freeze drying. CEL nanosuspensions were dried with no addition of sugars and surfactants.

Table 3. CEL nanosuspensions.

Formulation				***w/w* Ratio**	**Particle Size (nm) ***
		Stabilizer	**Surfactant**		
No.					
1	**CEL**	β-cyclodextrin	SLS	1:1:1	747.3 ± 21.09
2		PVP K 12	SLS	1:3:2	705.2 ± 28.52
3		PVP K 30	SLS	1:1:1	889.6 ± 55.64
4		PVA	Tween 80	1:2:1	863.0 ± 41.79
5		HPMC	Tween 80	1:3:2	960.9 ± 22.51

* Data are presented as mean ± standard deviation.

3.3. Characterization of Dry CEL Nanoparticles

3.3.1. DSC Study

Raw CEL has a sharp, distinct endothermic peak at 162.51 °C. All spray-dried and freeze-dried formulations 1–5 exhibited melting points ranging from 157.46 to 164.25 °C. No incompatibilities were detected in the obtained endothermic peaks and/or values of enthalpy in the thermograms of the studied formulations except spray-dried formulation 5 with a slight broader peak (Figure 1). The sample's melting point was the lowest at 157.46 °C, suggesting that the addition of Tween 80 and HPMC might have induced the formation of an amorphous state of CEL.

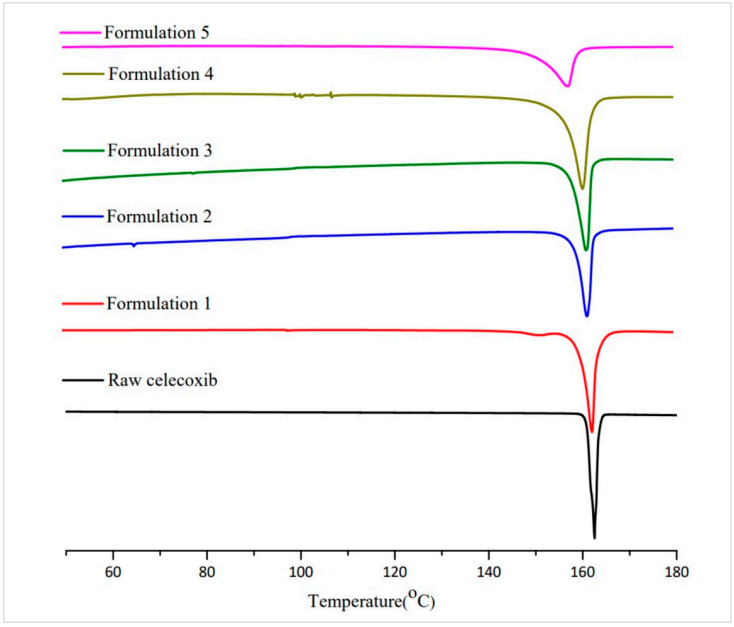

(**a**)

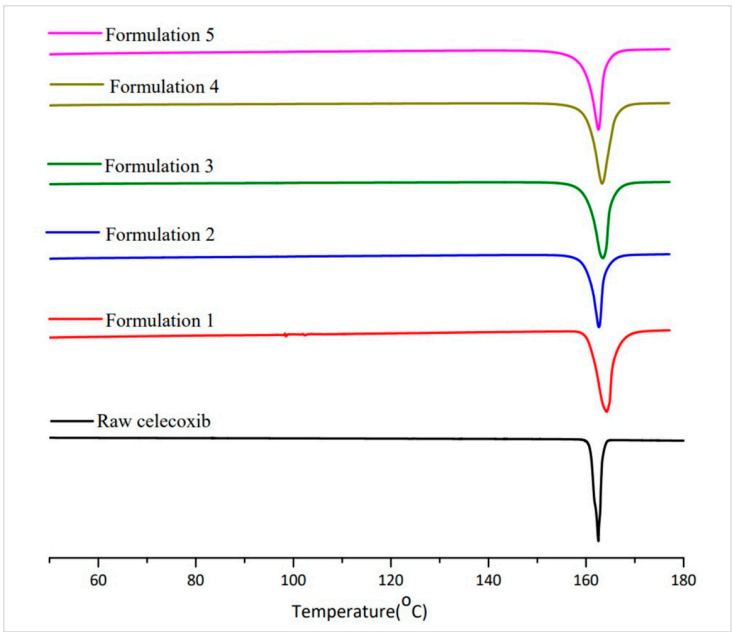

(**b**)

Figure 1. Differential Scanning Calorimetry (DSC) thermograms of (**a**) raw Celecoxib (CEL) and spray-dried formulations 1–5; (**b**) raw CEL and freeze-dried formulation 1–5.

3.3.2. ATR FTIR Study

The FTIR spectrum of raw CEL revealed absorption bands at 794.75, 1129.72, 1345.97, 1560.65, and 3333.22 cm^{-1}, which correspond to the drug's aromatic –CH bond, S=O symmetric and asymmetric bonds, and –NH and $–NH_2$ stretching. The CEL peaks are visible in all the dried samples' spectra (Figure 2). No evidence (shifting and broadening of peaks) of any bond formation was observed in the FTIR results, showing no chemical interaction involved between raw CEL and stabilizers and/or surfactants during the process of drying regardless of the different methods. Figure 1a shows the more intense 1560 cm^{-1} peaks of formulations 2 and 3; on the other hand, the 1560 cm^{-1} peaks in the corresponding freeze-dried formulations in Figure 1b are not as strong. This can be explained by the effect of PVP on the dissociation of cocrystals prepared by spray drying [21].

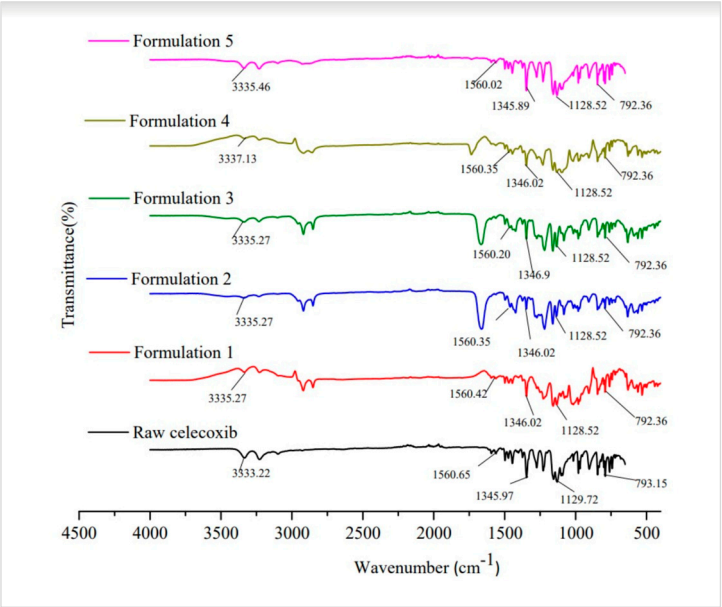

(**a**)

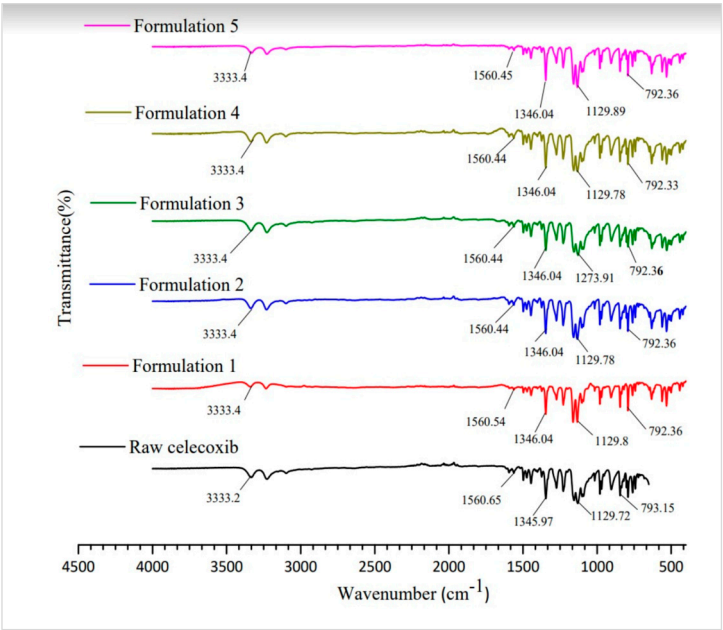

(**b**)

Figure 2. ATR FTIR results of (**a**) raw CEL and spray-dried formulations 1–5; (**b**) raw CEL and freeze-dried formulation 1–5.

3.3.3. PXRD Study

PXRD analysis was performed for raw CEL and powder formulations 1–5. CEL originally showed sharp peaks at 14.88°, 16.12°, and 19.68° in the PXRD results. Diffraction peaks originating from CEL crystals were observed in all formulations, indicating that the CEL nanoparticle powders did not have any new pattern of the crystal lattice and bond peaks that differed from CEL. The freeze-dried samples had a similar pattern to raw CEL, confirming their crystalline nature; meanwhile, the spray-dried formulations exhibited wider peaks at the degrees mentioned, indicating the slight conversion of crystallinity into an amorphous form due to the impact of high temperature (Figure 3).

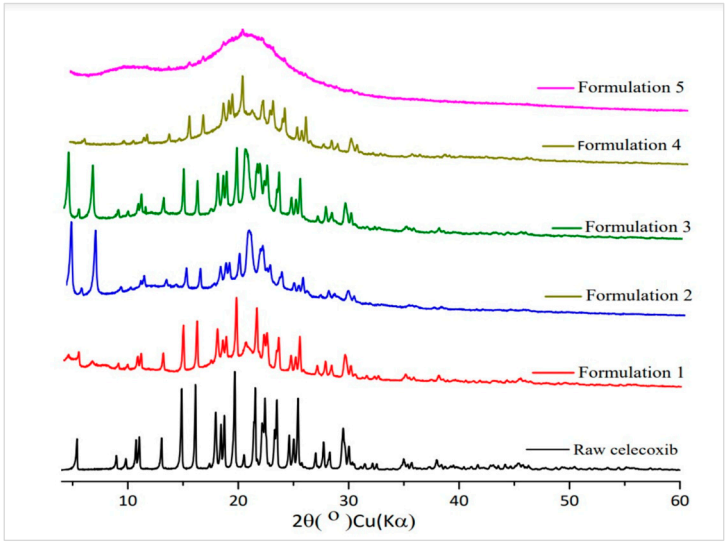

(**a**)

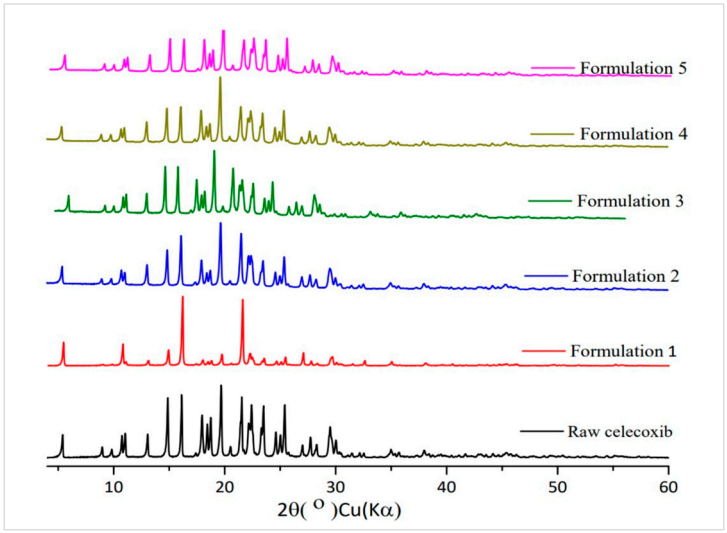

(**b**)

Figure 3. PXRD results of (**a**) raw CEL and spray-dried formulations 1–5; (**b**) raw CEL and freeze-dried formulation 1–5.

In agreement with the DSC results, spray-dried formulation 5 was confirmed to be in an amorphous state with no distinct peaks due to the lack of a defined crystal structure, which can be explained by the presence of HPMC in the formulation (Figure 3a). In addition, PVP is considered thermally stable, and thus formulations 2 and 3 show no significant difference in the DSC, ATR FTIR, and PXRD analysis results regardless of the different methods of drying. The advantages of spray drying are a short drying time and a stable final product [22]. PVP is an inert soluble polymer that can help increase the dissolution rate and solubility of drugs by inhibiting the growth of crystals in the transformation phase, resulting in the shift to the right of the diffractograms of formulations 2 and 3 at 6–7 degrees 2θ which appears in Figure 3a and could represent the growth of crystals.

3.3.4. SEM Analysis

The SEM-characterized morphology of raw CEL powder is shown in Figure 4. Raw CEL crystals appear to be long particles with sharp corners. Raw CEL particle size ranges from 1 to 10 μm, which correlates with the assessment of particle size reported previously [1,4,5].

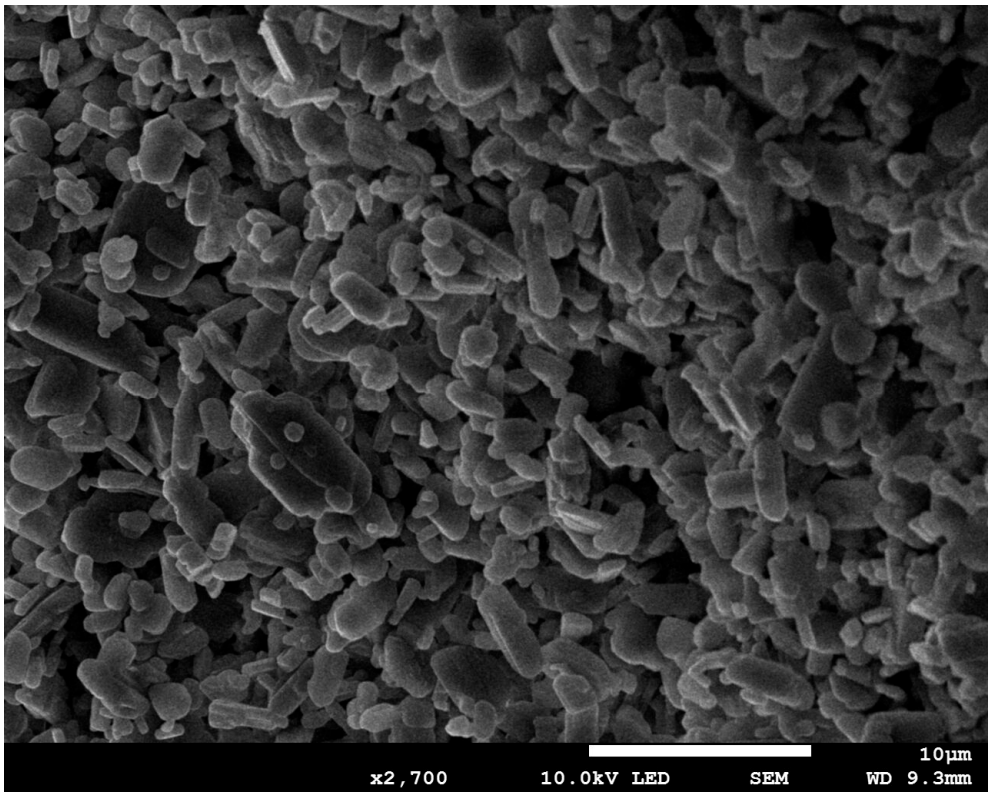

Figure 4. SEM picture of raw CEL powder.

In order to observe the morphology of dried nanosuspension CEL powder, SEM imaging of freeze-dried formulations 1–5 was performed, and then SEM pictures of spray-dried formulations 1, 4, and 5—the formulations with the highest amorphous level—were obtained. As shown in Figure 5a–e, formulations 1–3 with SLS as a surfactant exhibited a round shape, with particle size ranging from 1 to 30 µm. Meanwhile, formulations 4 and 5 with Tween 80 as a surfactant exhibited an irregular amorphous formation with undefined shape and particle size values varying from 1 to 50 µm. This micrographic particle size analysis agreed with the results measured by DLS (Table 2), thus confirming that the nanoparticle morphology was influenced by the choice of stabilizers. The CEL nanosuspension stabilized with PVA and Tween 80 showed stickiness characteristics (Figures 5d and 6b) [23]. In agreement with the DSC and PXRD results, HPMC adheres strongly to CEL nanoparticle surfaces and its adhesive strength increases with temperature; thus, spray-dried formulation 5 (Figure 6c) appears to be smoother compared to freeze-dried formulation 5 (Figure 5e).

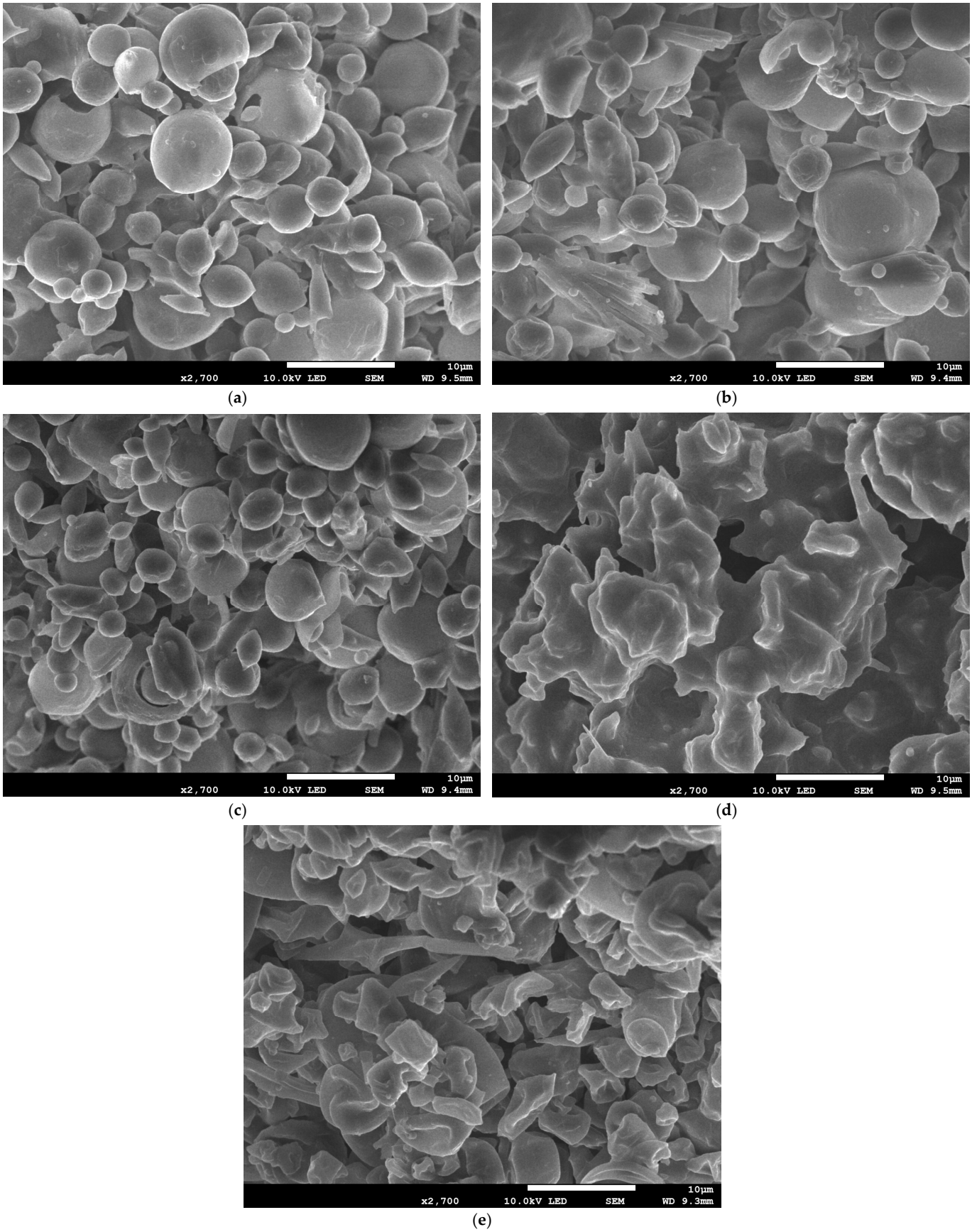

Figure 5. SEM picture of (**a**) freeze-dried formulation 1; (**b**) freeze-dried formulation 2; (**c**) freeze-dried formulation 3; (**d**) freeze-dried formulation 4; (**e**) freeze-dried formulation 5.

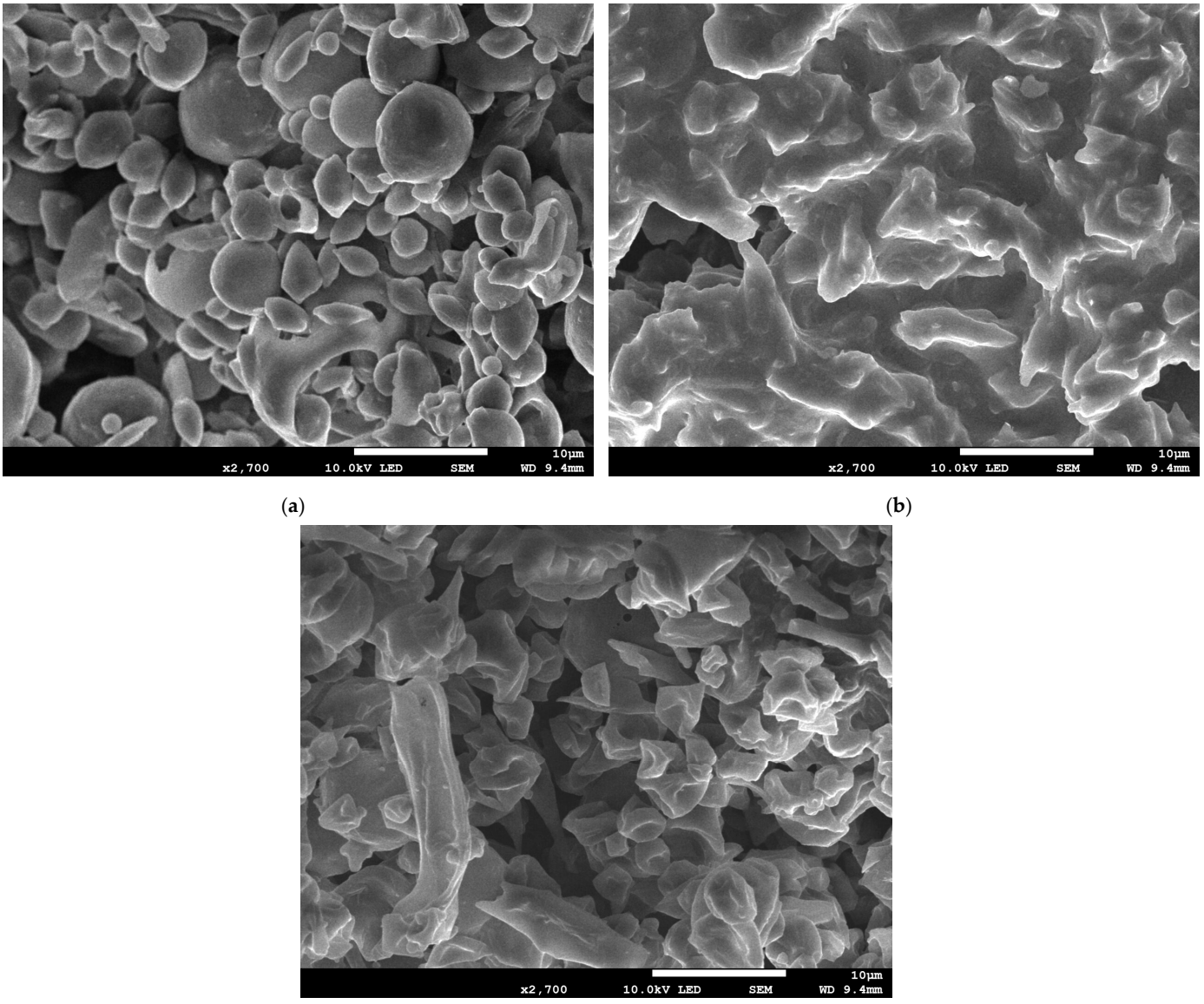

(**a**) (**b**)

(**c**)

Figure 6. SEM picture of (**a**) spray-dried formulation 1; (**b**) spray-dried formulation 4; (**c**) spray-dried formulation 5.

3.3.5. Dissolution Study

The release of CEL from the spray-dried and freeze-dried formulations in 0.1 M HCl with 0.2% SLS dissolution media and SLS-free dissolution media was performed, and the in vitro drug release profiles of CEL from raw CEL in comparison with CEL from the formulations are shown in Figure 7. There was almost no dissolution of CEL from raw CEL in the first 20 min in SLS-free dissolution media. The release rate of CEL from the tested formulations in the first 20 min was determined to be in the following order: freeze-dried formulation 5 > freeze-dried formulation 1 > freeze-dried formulation 2 > freeze-dried formulation 3 > freeze-dried formulation 4 > raw CEL and spray-dried formulation 2 > spray-dried formulation 1 > spray dried formulation 3 > spray-dried formulation 5 > spray-dried formulation 4 > raw CEL. The freeze-dried nanosuspension showed a slight delay in the first 20 min compared to the spray-dried nanosuspension. After the initial stage, dissolution progressed with a lag phase that represents aggregation affecting to all formulations.

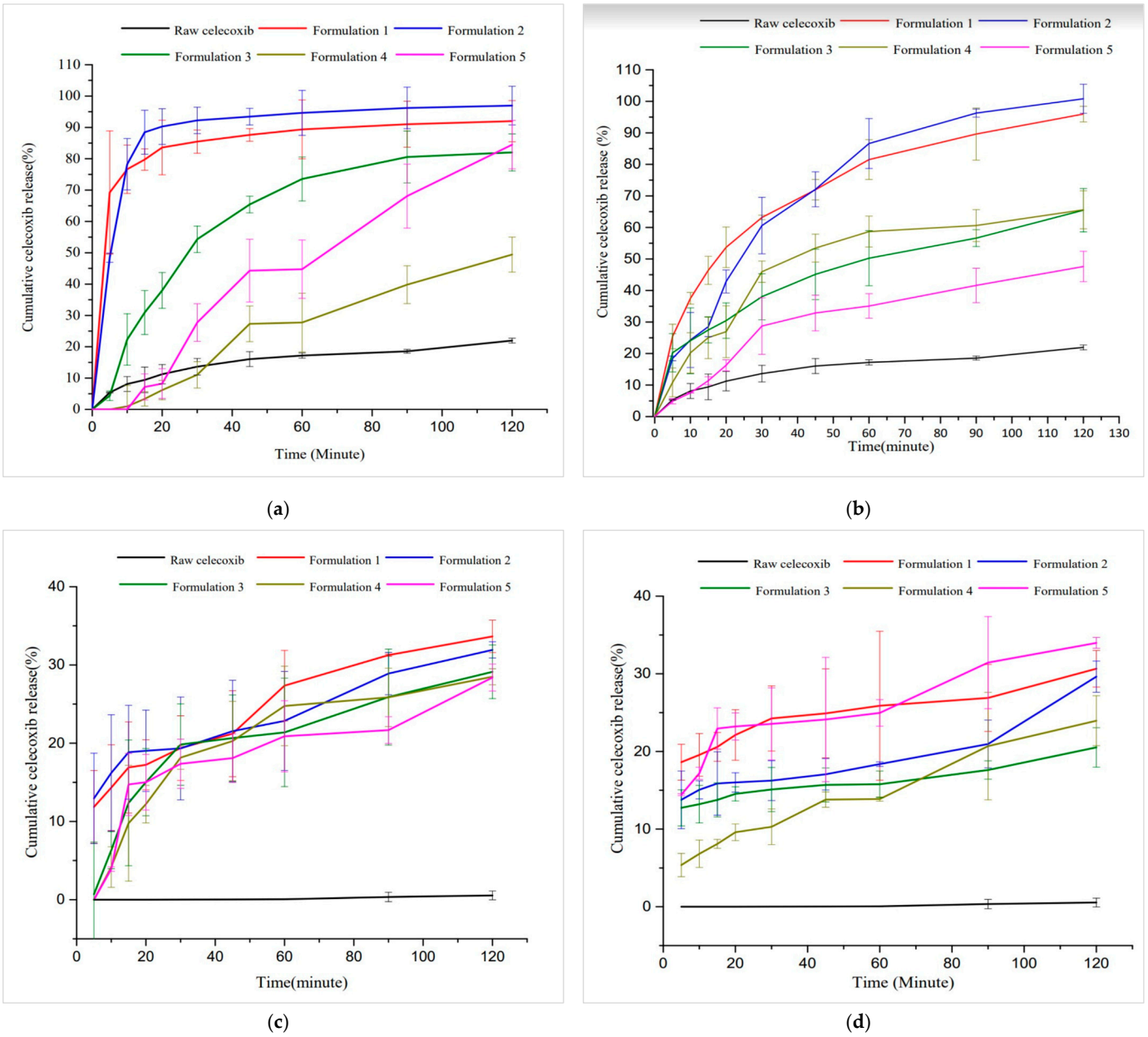

Figure 7. Dissolution profiles of (**a**) raw CEL and spray-dried formulations 1–5 in 0.1 M HCl with 0.2% SLS dissolution media; (**b**) raw CEL and freeze-dried formulations 1–5 in 0.1 M HCl with 0.2% SLS dissolution media; (**c**) raw CEL and freeze-dried formulations 1–5 in SLS-free dissolution media; (**d**) raw CEL and spray-dried formulations 1–5 in SLS-free dissolution media.

Drug release from the formulations increased significantly compared to raw CEL in both dissolution conditions. In SLS-free dissolution media, less than 1% of CEL was released from the raw CEL, whereas spray-dried and freeze-dried formulations 1–5 showed a release of 20.5–34% of CEL. In 0.1 M HCl with 0.2% SLS dissolution media, approximately 22% of CEL was released from raw CEL. After 2 h, 96% of CEL was released from freeze-dried formulation 1 and 100% of CEL was released from freeze-dried formulation 2. A total of 92.3% of CEL was released from spray-dried formulation 1, while 97% of CEL was released from spray-dried formulation 2. Figure 7d presents the in vitro drug release study results of the spray-dried formulations in SLS-free dissolution; interestingly, spray-dried formulation 5 with the highest amorphous degree exhibited the fastest release rate and 28.4% of CEL was released after 120 min. The results agree with the fact that SLS promoted CEL dissolution by promoting the crystallization of CEL and the dissolution of CEL in

amorphous form [1]. In addition, nanosuspensions with a nanosized particle size solve the problem of the poor aqueous solubility of CEL. In our previous study, the raw CEL particle size was 1.74–8.97 μm [5]; reducing the particle size of CEL nanoparticles significantly improved CEL solubility, although particle size data of the dried CEL nanoparticles are not shown in this article.

The initial dissolution of dry powders in dissolution media (0.1 M HCl with 0.2% SLS) was observed. Powdered formulations showed aggregation, indicating that the drying of CEL nanosuspensions led to the formation of aggregates. It is worth noting that surfactants and sugars were not added to the nanosuspensions during both drying processes since sugars could lead to a higher particle size after spray drying compared to the original nanosuspensions [14]. Although CEL nanoparticles were not stabilized during drying, there was no presence of larger particle aggregates seen after drying and sieving. The use of stabilizers and surfactants in the preparation of CEL nanosuspensions was sufficient to stabilize CEL nanoparticles. Formulations 1–3 with SLS (anionic surfactant) dispersed better compared to formulations 4 and 5 with Tween 80, which has a neutral charge. The absence of surface charge makes it difficult for the CEL particle aggregates to redisperse.

4. Conclusions

CEL nanosuspensions were successfully formulated using the antisolvent precipitation technique followed by high-pressure homogenization, and then subjected to drying processes in order to create dry powders for capsules for oral administration. The resulting CEL nanoparticles exhibited significantly improved dissolution profiles compared to raw CEL, suggesting that this formulation approach can enhance the bioavailability of CEL. Both spray drying and freeze drying were found to be effective methods for drying the nanosuspensions. Hence, this study demonstrates the potential of nanosuspension technology and drying nanosuspensions for capsules for oral administration to improve CEL solubility and ultimately its bioavailability and efficacy. Further research is needed to evaluate the in vivo performance of these nanosuspensions and to explore their potential applications in various clinical settings.

Author Contributions: Conceptualization, L.D.; methodology, L.D.; software, R.M.; validation, R.M. and L.D.; formal analysis, L.D.; investigation, R.M.; resources, S.-J.H.; data curation, R.M.; writing—original draft preparation, R.M.; writing—review and editing, L.D.; visualization, R.M.; supervision, S.-J.H.; project administration, S.-J.H.; funding acquisition, S.-J.H. All authors have read and agreed to the published version of the manuscript.

Funding: This work was supported by the Mid-Career Researcher Program (No. NRF-2021R1A2C2008834) and the Basic Research Infrastructure Support Program (University-Centered Labs-2018R1A6A1A03023718) through the National Research Foundation of Korea (NRF) funded by the Korean government (MSIT).

Institutional Review Board Statement: Not applicable.

Informed Consent Statement: Not applicable.

Data Availability Statement: Data is contained within the article.

Acknowledgments: The authors express their gratitude to Jong-Ju Lee, Jooseung Lee, and other lab colleagues who were always ready to help during the experiments. The authors appreciate all the support received from Bingfang Yan and his team and the Advanced Materials Characterization Center core facility within the College of Engineering and Applied Science, University of Cincinnati USA.

Conflicts of Interest: The authors declare no conflicts of interest.

References

1. Dinh, L.; Choi, J.; Machamasi, R.; Lee, J.-J.; Kim, M.; Hwang, S.-J. Preparation and characterization of intramuscularly long-acting celecoxib nanosuspensions for postoperative pain management. *J. Pharm. Investig.* **2024**. [CrossRef]
2. Gong, L.; Thorn, C.F.; Bertagnolli, M.M.; Grosser, T.; Altman, R.B.; Klein, T.E. Celecoxib pathways: Pharmacokinetics and pharmacodynamics. *Pharmacogenet Genom.* **2012**, *22*, 310–318. [CrossRef] [PubMed]

3. Bąk, U.; Krupa, A. Challenges and Opportunities for Celecoxib Repurposing. *Pharm. Res.* **2023**, *40*, 2329–2345. [CrossRef] [PubMed]
4. Hyun, S.-M.; Lee, B.J.; Abuzar, S.M.; Lee, S.; Joo, Y.; Hong, S.-H.; Kang, H.; Kwon, K.-A.; Velaga, S.; Hwang, S.-J. Preparation, characterization, and evaluation of celecoxib eutectic mixtures with adipic acid/saccharin for improvement of wettability and dissolution rate. *Int. J. Pharm.* **2019**, *554*, 61–71. [CrossRef]
5. Hong, S.-H.; Dinh, L.; Abuzar, S.M.; Lee, E.S.; Hwang, S.-J. Synthesis of Celecoxib-Eutectic Mixture Particles via Supercritical CO_2 Process and Celecoxib Immediate Release Tablet Formulation by Quality by Design Approach. *Pharmaceutics* **2022**, *14*, 1549. [CrossRef]
6. Arslan, A.; Yet, B.; Nemutlu, E.; Akdağ Çaylı, Y.; Eroğlu, H.; Öner, L. Celecoxib Nanoformulations with Enhanced Solubility, Dissolution Rate, and Oral Bioavailability: Experimental Approaches over In Vitro/In Vivo Evaluation. *Pharmaceutics* **2023**, *15*, 363. [CrossRef]
7. Dizaj, S.M.; Vazifehasl, Z.; Salatin, S.; Adibkia, K.; Javadzadeh, Y. Nanosizing of drugs: Effect on dissolution rate. *Res. Pharm. Sci.* **2015**, *10*, 95–108.
8. Lee, J.; Lee, J.J.; Lee, S.; Dinh, L.; Oh, H.; Abuzar, S.M.; Ahn, J.H.; Hwang, S.J. Preparation of Apixaban Solid Dispersion for the Enhancement of Apixaban Solubility and Permeability. *Pharmaceutics* **2023**, *15*, 907. [CrossRef]
9. Shaji, J.; Lodha, S. Response Surface Methodology for the Optimization of Celecoxib Self-microemulsifying Drug delivery System. *Indian J. Pharm. Sci.* **2008**, *70*, 585–590. [CrossRef]
10. Lee, J.J.; Dinh, L.; Park, J.; Khraisat, R.; Park, J.W.; Jeong, J.K.; Lee, J.; Kim, H.S.; Park, M.S.; Ahn, J.H.; et al. Preparation and characterization of lysozyme loaded liposomal dry powder inhalation using non-ionic surfactants. *Int. J. Pharm.* **2023**, *646*, 123426. [CrossRef]
11. Kang, H.; Cha, K.H.; Cho, W.; Park, J.; Park, H.J.; Sun, B.K.; Hyun, S.M.; Hwang, S.J. Cyclosporine Amicellar delivery system for dry eyes. *Int. J. Nanomed.* **2016**, *11*, 2921–2933.
12. Liu, Y.; Liang, Y.; Yuhong, J.; Xin, P.; Han, J.L.; Du, Y.; Yu, X.; Zhu, R.; Zhang, M.; Chen, W.; et al. Advances in Nanotechnology for Enhancing the Solubility and Bioavailability of Poorly Soluble Drugs. *Drug Des. Devel. Ther.* **2024**, *18*, 1469–1495. [CrossRef]
13. Wu, C.Y.; Wang, W. Application of Antisolvent Precipitation Method for Formulating Excipient-Free Nanoparticles of Psychotropic Drugs. *Pharmaceutics* **2022**, *14*, 819. [CrossRef]
14. Chaubal, M.V.; Popescu, C. Conversion of nanosuspensions into dry powders by spray drying: A case study. *Pharm. Res.* **2008**, *25*, 2302–2308. [CrossRef] [PubMed]
15. Mudie, D.M.; Amidon, G.L.; Amidon, G.E. Physiological parameters for oral delivery and in vitro testing. *Mol. Pharm.* **2010**, *7*, 1388–1405. [CrossRef] [PubMed]
16. Luner, P.E.; Vander Kamp, D. Wetting behavior of bile salt-lipid dispersions and dissolution media patterned after intestinal fluids. *J. Pharm. Sci.* **2001**, *90*, 348–359. [CrossRef]
17. Jo, K.; Cho, J.M.; Lee, H.; Kim, E.K.; Kim, H.C.; Kim, H.; Lee, J. Enhancement of Aqueous Solubility and Dissolution of Celecoxib through Phosphatidylcholine-Based Dispersion Systems Solidified with Adsorbent Carriers. *Pharmaceutics* **2018**, *11*, 1. [CrossRef]
18. Zhao, X.; Wang, H.; Zhang, Z.; Jin, H.; Gong, Y. Effects of ethyl acetate extract of *Salsola collina* on brain-gut peptides and interstitial cells of gastric Cajal in rats with diabetic gastroparesis. *Iran J. Basic Med. Sci.* **2020**, *23*, 1218–1224.
19. Babu, R.J.; Dayal, P.; Singh, M. Effect of cyclodextrins on the complexation and nasal permeation of melatonin. *Drug Deliv.* **2008**, *15*, 381–388. [CrossRef]
20. Kurakula, M.; Rao, G.S.N.K. Pharmaceutical assessment of polyvinylpyrrolidone (PVP): As excipient from conventional to controlled delivery systems with a spotlight on COVID-19 inhibition. *Drug Deliv. Sci. Technol.* **2020**, *60*, 102046. [CrossRef]
21. Shao, S.; Stocker, M.W.; Zarrella, S.; Korter, T.M.; Singh, A.; Healy, A.M. In Situ Cocrystallization via Spray Drying with Polymer as a Strategy to Prevent Cocrystal Dissociation. *Mol. Pharm.* **2023**, *20*, 4770–4785. [CrossRef] [PubMed]
22. Piñón-Balderrama, C.I.; Leyva-Porras, C.; Terán-Figueroa, Y.; Espinosa-Solís, V.; Álvarez-Salas, C.; Saavedra-Leos, M.Z. Encapsulation of Active Ingredients in Food Industry by Spray-Drying and Nano Spray-Drying Technologies. *Processes* **2020**, *8*, 889. [CrossRef]
23. Pereira, G.G.; Figueiredo, S.; Fernandes, A.I.; Pinto, J.F. Polymer Selection for Hot-Melt Extrusion Coupled to Fused Deposition Modelling in Pharmaceutics. *Pharmaceutics* **2020**, *12*, 795. [CrossRef] [PubMed]